Thermodynamic modelling of the ternary Bi-Ga-Te system for potential application in thermoelectric materials

Bhupendra Kumar[a], Chandra Shekhar Tiwary[a], Min-Kyu Paek[b*], Manas Paliwal[a*]

[a]Department of Metallurgical and Materials Engineering, Indian Institute of Technology Kharagpur, 721302, West Bengal, India.

[b]Department of Chemical and Metallurgical Engineering, Aalto University, 02150, Espoo, Finland.

*Email: manas.paliwal@metal.iitkgp.ac.in

*Email: minkyupaek@gmail.com

Abstract

Thermoelectric materials have drawn widespread attention because they can enable the direct conversion between electric and thermal energy. Over the years, different materials such as skutterudites, clathrates, intermetallic alloys, eutectic alloys, chalcogenides have been explored for Thermoelectric (TE) applications. Amongst the eutectic alloys, the Bi-Ga-Te system exhibits promising potential as a TE material. Accordingly, in this study, we performed the thermodynamic optimization and critical evaluation of binary Bi-Ga, Bi-Te, Ga-Te, and ternary Bi-Ga-Te systems using the CALPHAD method. It is observed that the Ga-Te system shows asymmetric liquid solution properties with strong negative enthalpy of mixing, whereas the Bi-Te liquid exhibits the symmetric regular solution behavior. Moreover, the Bi-Ga liquid solution has a positive enthalpy of mixing. Therefore, Modified Quasichemical Model (MQM) using pair approximation was utilized to describe the diversified thermodynamic properties of liquid solution in sub-binaries by taking into account the Short-Range Ordering (SRO). By merging the binary optimization results with a proper interpolation method, the liquid solution properties and phase diagram information in the Bi-Ga-Te ternary system were also reproduced successfully without any adjustable ternary parameter. Several ternary eutectic compositions were suggested for designing TE alloy with enhanced properties using the developed database.

Keywords: Thermoelectric materials, Eutectic alloy, Bi-Ga-Te system, CALPHAD, Thermodynamic Optimization

Introduction

Thermoelectric (TE) materials have emerged as attractive materials for applications in various areas such as waste heat recovery and electronic cooling because of their ability to interchangeably convert thermal energy and electrical energy in a solid state [1,2]. Over the years, various materials such as skutterudites, clathrates, intermetallic alloys, chalcogenides have been explored for TE applications [3]. Bi_2Te_3-based alloys are the most commonly used materials for room temperature TE applications such as refrigeration and waste heat recovery up to 200 °C [1]. However, their efficiencies are not competitive enough with other alternative energy sources such as solar cells and fuel cells. Therefore, it is necessary to improve the performance of the TE materials.

The performance of thermoelectric materials is described by a dimensionless thermoelectric figure of merit (ZT) defined as: $S^2\sigma T/(k)$, where S, σ, k and T are Seebeck coefficient, electrical conductivity, thermal conductivity and temperature respectively. Seebeck coefficient of a material is defined as the ratio of an induced thermoelectric voltage to the temperature difference across that material [4]. It can be inferred from the Boltzmann transport equation that with increasing charge carrier, Seebeck coefficient should decrease [1,5]. But, the trend is reversed in electrical conductivity, as it is directly proportional to charge carrier [6]. Therefore, ZT maximization is difficult through Seebeck coefficient and electrical conductivity modification. Nano-structuring TE materials such as superlattices and quantum dots have been considered an effective way to increase the ZT due to their low thermal conductivity [7,8]. The low thermal conductivity of materials is associated with the enhanced phonon scattering by

nanoscale interfaces, either grain boundary or hetero-phase interfaces [7]. However, the production of such nanostructured materials comes with high cost and difficulties associated with scaling up the process, therefore the exploration of new methods is underway.

Multi-functional properties such as lower melting temperature, good mechanical and chemical properties, and low thermal conductivity of eutectic alloys are useful for various engineering applications [9–13]. In addition, eutectic alloys' lamellar structure resembles superlattice structure and thus are promising candidates for TE materials. In recent years, many eutectic alloys have been explored for TE applications such as PbTe-Sb_2Te_3 [14], PbTe-Bi_2Te_3 [15], PbTe-Si [16], Ag_2Te-PbTe-Sb_2Te_3 [17], PbTe-Te-Ag_5Te_3 [18], $(Bi,Sb)_2Te_3$-Te [19], GeTe-Ag_8GeTe_6 [20], InSb-Sb [21], Bi_2Te_3-In_2Te_3 [22], SnTe-Te [23]. These studies have reported improved ZT of the TE materials as eutectic structure lowers the thermal conductivity by enhancing phonon scattering. Further, a study shows that Ga in the Bi-Te system increases the carrier mobility due to the formation of additional energy level close to conduction band for n-type Bi_2Te_3 or close to valance band for p-type [24]. A recent study has reported ZT value 1.2-1.5 at 300 K in Ga-Bi-Te alloy [25]. Eutectic alloys in this system have not been explored for TE application. Therefore, in this study, we report the complete thermodynamic assessment of the Bi-Ga-Te system by simultaneously reproducing the thermodynamic and phase diagram data through critical evaluation of experimental data and adopting an appropriate model that accurately describes the structure of the liquid and solid phases. The thermodynamic calculations using this work will aid in designing new ternary eutectic compositions in the Bi-Ga-Te system.

To the best knowledge of the present authors, no thermodynamic optimization has been reported in the Bi-Ga-Te ternary system. In the present study, a thermodynamic investigation of

the ternary Bi-Ga-Te and its sub-binary systems was carried out. It is observed that liquid solution of Ga-Te and Bi-Te show strong and moderate negative mixing enthalpy, respectively, whereas the Bi-Ga liquid exhibits the positive deviation. Because of distinct binary liquid solution property, each binary system has been optimized using different solution model such as regular solution model, associate model, ionic model. In order to have thermodynamic consistency for the ternary extension, the Modified Quasichemical Model (MQM)[26,27] was used for the description of liquid solution properties. This model is flexibly considering such diversified nature of the three sub binary systems by adopting a pair exchange reaction. The Short-Range Ordering (SRO) exhibiting in the liquid solution was effectively accounted to describe the strong affinity of Te with Ga and Bi as well as positive deviation of liquid Bi-Ga. The Compound Energy Formalism (CEF) was used to explain the solid solution properties [28]. Gierlotka's [29] results for the solid phases in the Bi-Te system were mainly adopted, however, some model parameters were slightly revised to reproduce the overall consistency of phase diagram data. The heat capacity function of intermetallic compounds GaTe and Ga_2Te_3 were redefined from the available experimental findings [30–32]. The heat capacity of Ga_3Te_4 was derived from the newly defined heat capacity of GaTe and Ga_2Te_3, and that of Ga_2Te_5 was derived from the constituent elements in their reference state. Combining the optimized model parameters of the three sub-binary systems, Gibbs free energy of ternary liquid solution was estimated by taking a reasonable interpolation method.

1. Thermodynamic models

All the calculations and optimization in the present study were performed using FactSage thermochemical software [33,34]. The Gibbs free energies of all phases of pure Ga, Bi, and Te were taken from Dinsdale [35].

2.1 Pure elements and stoichiometric compound

The Gibbs free energies of all pure elements were taken from Scientific Group Thermodata Europe (SGTE) database and the Gibbs free energies of pure compounds were determined based on the available experimental data such as heat capacity, standard enthalpy, and entropy at 298.15 K. As the thermodynamic principle, the Gibbs free energies of pure elements can be calculated as follows:

$$G_T^\circ = H_T^\circ - TS_T^\circ \quad (1)$$

$$H_T^\circ = H_{298.15\,K}^\circ + \int_{298.15\,K}^{T} C_p dT \quad (2)$$

$$S_T^\circ = S_{298.15\,K}^\circ + \int_{298.15\,K}^{T} (C_p/T) dT \quad (3)$$

where $H_{298.15\,K}^\circ$, $S_{298.15\,K}^\circ$, and C_p are standard enthalpy of formation from the stable pure elements at 298.15 K, entropy of formation at 298.15 K and heat capacity, respectively. The heat capacity expression of each compound can be determined by fitting heat capacity data. In case of no available reliable data on C_p, Neumann-Kopp rule [36] was used to predict the C_p expression.

2.2 Liquid solution

Modified Quasichemical Model (MQM) [26][27] which accounts for the short-range ordering of the nearest neighbor atoms was used to describe the liquid solutions. Compared to the conventional Bragg-Williams Random Mixing Model, the MQM gives a more realistic description of the entropy of the solution. In the MQM, Gibbs energy of a pair formation can be expressed in a polynomial of a pair fraction instead of a component fraction. Besides, the coordination number is allowed to vary with the composition. These added features of the MQM provide greater flexibility in reproducing the binary experimental data and combining optimized binary liquid parameters into a larger database for a multicomponent system.

In the MQM, the reaction of pair exchanging in a binary *A-B* liquid solution can be expressed by the distribution of *A* and *B* atoms over the sites of the quasi lattice as follows:

$$(A-A)+(B-B)=2(A-B);\ \Delta g_{AB} \tag{4}$$

where (*i-j*) represents the First-Nearest Neighbor (FNN) pair between components *i* and *j*, and Δg_{AB} is the Gibbs energy change of forming two moles of (*A-B*) pairs. The Gibbs energy of the liquid solution can be calculated by the following equation:

$$G_L^{sol} = n_A \overset{\circ}{g}_A + n_B \overset{\circ}{g}_B - T\Delta S^{config} + \left(\frac{n_{AB}}{2}\right)\Delta g_{AB} \tag{5}$$

where n_A, n_B and n_{AB} are the moles of *A*, *B*, and (*A-B*) pair, respectively. $\overset{\circ}{g}_A$ and $\overset{\circ}{g}_B$ are the molar Gibbs energies of the pure A and B components. ΔS^{config} is the configurational entropy of randomly mixing (*A-A*), (*B-B*), and (*A-B*) pairs.

$$\Delta S^{config} = -R\left(n_A \ln X_A + n_B \ln X_B\right) - R\left(\left(n_{AA} \ln \left(\frac{X_{AA}}{Y_A^2}\right) + n_{BB} \ln \left(\frac{X_{BB}}{Y_B^2}\right) + n_{AB}\right.\right. \tag{6}$$

where n_{ij} is the number of moles of (*i-j*) pairs. Z_A and Z_B are the coordination numbers of *A*

and B, respectively. Pair fraction X_{ii}, mole fraction X_i, and coordination equivalent fraction Y_i are defined as follows:

$$X_{ii} = \frac{n_{ii}}{(n_{AA}+n_{BB}+n_{AB})} \tag{7}$$

$$X_A = \frac{n_A}{n_A+n_B} = 1 - X_B \tag{8}$$

$$Y_A = \frac{Z_A n_A}{Z_A n_A+Z_B n_B} = 1 - Y_B \tag{9}$$

$$Z_i n_i = 2n_{ii} + n_{AB} \tag{10}$$

Equation (10) can be obtained by mass balance of (i-j) pairs. The Δg_{AB} is the model parameter and can be expanded as a polynomial in terms of the pair fraction as follows:

$$\Delta g_{AB} = \Delta g^{\circ}_{AB} + \sum_{i\geq 1} \Delta g^{i0}_{AB} X^i_{AA} + \sum_{j\geq 1} \Delta g^{0j}_{AB} X^j_{BB} \tag{11}$$

Δg°_{AB}, Δg^{i0}_{AB} and Δg^{0j}_{AB} are the model parameters, and that can be a function of temperature. The composition dependent coordination numbers are given as follows:

$$\frac{1}{Z_A} = \frac{1}{Z^A_{AA}}\left(\frac{2n_{AA}}{2n_{AA}+n_{AB}}\right) + \frac{1}{Z^A_{AB}}\left(\frac{2n_{AB}}{2n_{AA}+n_{AB}}\right) \tag{12}$$

$$\frac{1}{Z_B} = \frac{1}{Z^B_{BB}}\left(\frac{2n_{BB}}{2n_{BB}+n_{AB}}\right) + \frac{1}{Z^B_{BA}}\left(\frac{2n_{AB}}{2n_{AA}+n_{AB}}\right) \tag{13}$$

where Z_{AA} is the value Z_A when all nearest-neighbor atoms of atom A are atoms A, and Z_{AB} is the value of Z_A when all nearest neighbors are B atoms. Z_{AB} and Z_{BA} are defined

analogously. The composition of maximum SRO in each binary subsystem is estimated by ratio of the coordination numbers Z_B/Z_A. In this study, Z_{ij} (*i, j* = Bi, Ga, Te) are set to 6, except $Z_{GaTe} = 4$. This change in coordination number was made to consider the asymmetry of liquid solution with the maximum SRO near X_{Te} = 0.6 in the binary Ga-Te system.

The Gibbs energy of the ternary liquid solution can be predicted based on the model parameter of the sub binary systems. One of the advantages of the MQM is the flexibility to choose the interpolation method depending on the nature of each binary liquid solution [37]. Toop-like interpolation with Te as an asymmetric component was used to describe the asymmetry of the ternary liquid with the positive enthalpy of mixing in the Bi-Ga system and the negative enthalpy of mixing in the Bi-Te and Ga-Te systems.

2.3 Solid solution

The Compound Energy Formalism (CEF) [28] is used to describe the Gibbs energies of the solid solutions in the Bi-Ga-Te system such as β and Bi_2Te_3 phases considering their crystal structures of rhombohedral and Body-Centered Tetragonal (BCT), respectively. In the CEF, a solid solution composed of two kinds of sublattices such as substitutional and interstitial sites $(A,\ B)_n(C,\ D)_m$. The Gibbs energy of the solid solution can be expressed as:

$$G_s^{sol.} = y_A^{'} y_C^{''} G_{A:C} + y_A^{'} y_D^{''} G_{A:D} + y_B^{'} y_C^{''} G_{B:C} + y_B^{'} y_D^{''} G_{B:D} + nRT\left(y_A^{'} lny_A^{'} + y_B^{'} lny_B^{'}\right)$$

$$+ \; mRT\left(y_C^{''} ln y_C^{''} + y_D^{''} ln y_D^{''}\right) + \sum_{i,j,k} y_i^{'} y_j^{'} y_k^{''} L_{i,j:k} + \sum_{i,j,k} y_k^{'} y_i^{''} y_j^{''} L_{k:i,j} \qquad (14)$$

where $y_i^{'}$ and $y_i^{''}$ are the site fraction of species *i* in the corresponding sublattice. $G_{i:j}$ is the Gibbs free energy of an end-member, the $L_{i,j:k}$ and $L_{k:i,j}$ are adjustable interaction parameters between the component *i* and *j* on one sublattice when the other sublattice is occupied by k.

In the Bi-Ga-Te ternary system, there are only two existing solid solution phases, β and Bi_2Te_3. The β phase is described as the orderly stacked unit of Bi and Bi_2Te_3, thus, it was formulated as $(Bi)_2(Bi, Te)_3$ [38]. Small homogeneity range at high temperature in intermetallic compound Bi_2Te_3 is described as anti-site defects and it is described as $(Bi, Te)_2(Bi, Te)_3$ adopted from the previous assessment [29]. Self-consistent thermodynamic parameter from the present optimization is given in Table 1.

Table 1: Optimized model parameter of the Bi-Ga-Te system

Liquid	**MQM[(a)] (Bi,Ga,Te)**
$Z_{BiBi}^{Bi} = Z_{GaGa}^{Ga} = Z_{TeTe}^{Te} = Z_{BiGa}^{Bi} = Z_{BiGa}^{Ga} = Z_{BiTe}^{Bi} = Z_{BiTe}^{Te} = Z_{GaTe}^{Ga} = 6;\ Z_{GaTe}^{Te} = 4;$	
$\Delta g_{BiGa} = 3050 - 0.15T + (1020 + 0.3T)X_{GaGa} - 950X_{BiBi}^{3}$	
$\Delta g_{BiTe} = -10340 + 3T + (-2500 + 0.7T)X_{TeTe}$	
$\Delta g_{GaTe} =$	
$-39950 + 15.22T + (20200 - 13.6T)X_{GaGa} + 8300X_{GaGa}^{2} + 9900X_{TeTe} - 4$	

$g^{001}_{BiGa(Te)} = 0$

β phase	CEF[(b)] $(Bi)_2(Bi, Te)_3$
	$G_{Bi:Bi} = 5\,{}^{\circ}G^{SER}_{Bi} + 6071.29 + 13T$
	$G_{Bi:Te} = 2\,{}^{\circ}G^{SER}_{Bi} + 3\,{}^{\circ}G^{SER}_{Te} - 83773.19$
	$L_{Bi:Bi,Te} = -45563.5 - 20.4T$

Bi_2Te_3	CEF[(b)] $(Bi, Te)_2(Bi, Te)_3$
	$G_{Bi:Bi} = 5\,{}^{\circ}G^{SER}_{Bi} + 150000$
	$G_{Bi:Te} = 2\,{}^{\circ}G^{SER}_{Bi} + 3\,{}^{\circ}G^{SER}_{Te} - 85735.54$
	$G_{Te:Bi} = 0$
	$G_{Te:Te} = 5\,{}^{\circ}G^{SER}_{Te} + 150000$
	$L_{Bi,Te:Bi} = L_{Bi,Te:Te} = 18000 - 145T$
	$L_{Bi:Bi,Te} = L_{Te:Bi,Te} = 5000 - 175T$

Intermetallic Compounds	
Bi_2Te	
${}^{\circ}G^{Bi_2Te} = -55913.22644 + 430.4017312T - 92.4880058T \ln ln(T) + 0.0405$	
$-5T^3$	(298<T<1200)
Bi_4Te_3	

$^{\circ}G^{Bi_4Te_3} = -151095.1298568 + 1044.5973421T - 220.644711T \ln ln(T) + 0$

$-5T^3$ (298<*T*<1400)

GaTe

$^{\circ}G^{GaTe} = -90741.7252602 + 109.9048882T - 22.84411T \ln ln(T) - 8.870$

$-2T^2 + 12806.9T^{-1} + 5E-5T^3$

(50<*T*<298)

$-92173.7944225 + 204.1644557T - 41.67499T\,ln(T) - 1.404396E-$

$2T^2 - 945.6965T^{-1} + 1.9558833E-6T^3$

(298<*T*<1600)

Ga_2Te_3

$^{\circ}G^{Ga_2Te_3} = -228100.4698815 + 415.3425275T - 86.77225T \ln ln(T) - 0.10805T^2 + 49661T^{-1} + 5.6666667E-5T^3$

(50<*T*<298)

$-230848.0085562 + 579.4559607T - 118.5T\,ln(T) - 0.0025T^2$

(298<*T*<1600)

Ga_3Te_4

$^{\circ}G^{Ga_3Te_4} = -327842.1951417 + 533.2474157T - 109.61636T \ln ln(T) - 0.196$

$-4T^3$ (50<*T*<298)

$-322021.8029788 + 791.6204165T - 160.17499T\,ln(T) - 0.0165439T^2 + 1.$

$-6T^3 - 945.6965T^{-1}$ (298<*T*<1600)

Ga_2Te_5

$^{\circ}G^{Ga_2Te_5} = -162080.15 + 31.7667852T + 2^{\circ}G_{Ga}^{SER} + 5^{\circ}G_{Te}^{SER}$ (298<*T*<1600)

[a] Modified Quasichemical Model
[b] Compound Energy Formalism
(All values are in J/mol)

3. Results and discussions

3.1 Bi-Ga Binary system

The phase diagram of the Bi-Ga is well known, and it shows a miscibility gap in the liquid phase with an upper critical temperature of about 530 K corresponding to an approximate composition of 70 at. % Ga. Neither mutual solid solubility between Bi and Ga nor intermetallic compounds have been reported in this system. The Bi-rich monotectic composition and temperature are 38.5 at. % Ga and 495 K, respectively. In the early study of this system, Girard et al. [39] have provided a thermodynamic dataset representing all the available experimental data of the system and carried out a critical assessment. Puschin et al.[40] reported the liquidus data using thermal analysis. Predel [41] reported the phase diagram using DTA analysis. Huber et al.[42] determined liquidus line using thermal and calorimetry analysis. Thermodynamic investigation of this system was performed by Jordan [43] and Manasijevic et al. [44]. The Bi-Ga liquid solution exhibits non-regular behavior as evident from the activity and positive heat of mixing of liquid solution. Therefore, Jordan [43] considered the random mixing of Bi, Ga, and dimeric Bi_2 molecules to describe the non-regular behavior of liquid Bi-Ga. They considered the dimeric Bi_2 molecules as some indirect evidence such as viscosity of Bi(l) calculated from kinetic theory agreed well with measured value when the molecular weight of Bi_2 was used, and moreover pair potential calculations for Bi(l) differ from typical monoatomic liquids. Manasijevic et al. [44] used a regular solution model for the

liquid phase, therefore, many adjustable model parameters were needed to describe the non-regular behavior of the liquid solution.

In the present study, the liquid solution was optimized using MQM to explicitly describe the non-ideal solution behavior in the Bi-Ga system. The calculated phase diagram along with experimental data is shown in figure 1. The phase diagram is in good agreement with the experimental data and previous assessment by Manasijevic et al. [44]. The calculated invariant reaction point (X_{Ga} = 0.36) at T = 495 K also corresponded well with the previous studies. Compared to previous assessments who used regular solution model, fewer model parameters were required to describe the liquid solution properties by using the MQM. The positive parameter of (Ga-Ga) pair was required to reproduce the liquid miscibility gap at the Ga-rich corner of the Bi-Ga phase diagram (Figure 1) as well as positive deviation of liquid solution properties as shown in figure 2 (a) and 2 (b). The third order parameter of (Bi-Bi) pair was added to fix the invariant reaction temperature and composition which were significantly affected by the positive parameter of (Ga-Ga) pair.

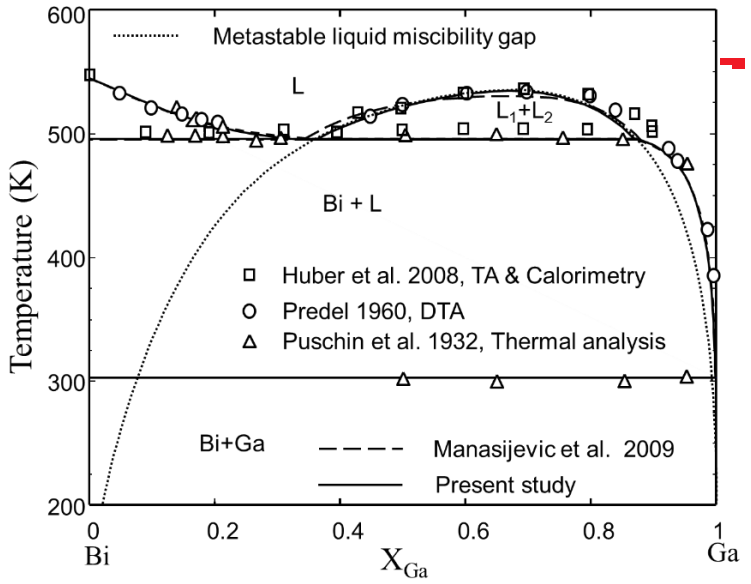

Figure 1 Calculated phase diagram of the Bi-Ga system by this work and Manasijevi et al. [44] *along with experimental data* [40–42].

Predel et al. [45] measured the activity of Ga in liquid at 583 K from the calorimetric measurements. Yatshenko and Danilin [46] and Katayama et al.[47] measured activity of Ga in the liquid phase using the EMF method between temperature 680-870 K and 1073 K, respectively. Yatshenko and Danilin used a mixture of KCl-LiCl and $GaCl_3$ as electrolytes while Katayama et al. employed solid Zr to measure the activity in the liquid phase. The enthalpy of mixing of the liquid Bi-Ga alloy was measured by Predel et al., [45] Gambino et al.[48], Moser and Rzyman [49], and Huber et al. [42] using high-temperature calorimetry. Zivkovic et al. [50] used DTA to measure the mixing enthalpy of the liquid phase at 545 K. The calculated activity and the mixing enthalpy of the liquid solution are shown in the figure 2 (a) and 2 (b), respectively. Calculated values are in good agreement with experimental data [42,45,48,50] except the activity data measured by EMF at temperature above 680 K.

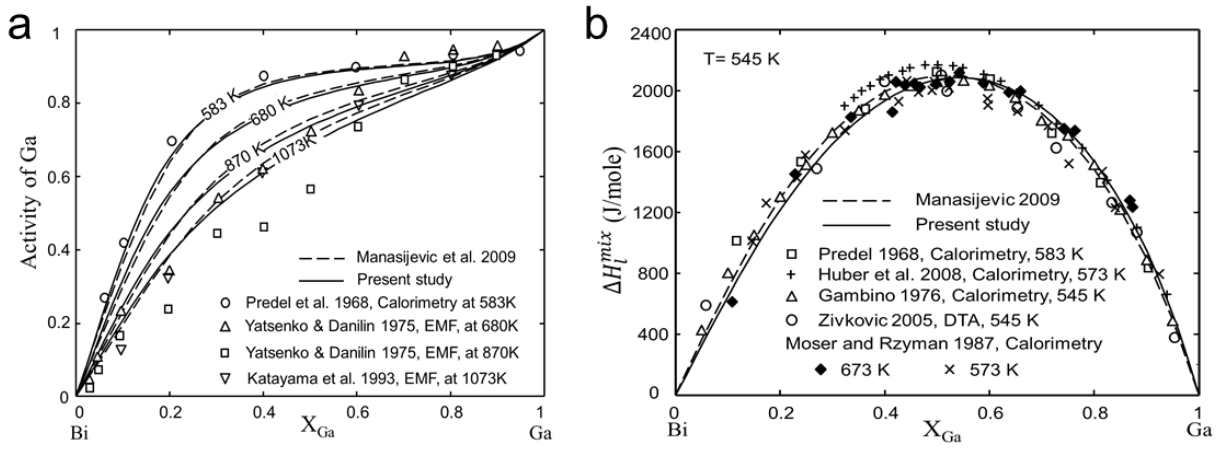

Figure 2 (a) Calculated activity of Ga(l) at 583, 680, 870 and 1073 K along with experimental data [45–47] *and (b) enthalpy of mixing in liquid Bi-Ga at 545 K along with experimental data* [42,45,48–50] *and previous calculation* [44]

3.2 Bi-Te system

Recently, Mao et al. [38] and Gierlotka [29] optimized the binary Bi-Te system. They have extensively reviewed the available thermodynamic and phase equilibrium data. According to their evaluations, there are two solution phases (liquid and β) and three stoichiometric compound phases (Bi_2Te, Bi_3Te_4, and Bi_2Te_3). Mao et al.[38] optimized liquid solution as a regular solution model based on the Redlich-Kister type polynomial series and solid phases of Bi_2Te_3, Bi_2Te, and Bi_4Te_3 as line compounds. Gierlotka [29] modified the system using the associate solution model for the liquid solution with Bi_2Te_3 as an associate and included high-temperature homogeneity range of thermoelectric phase Bi_2Te_3 reported by Brebrick [51]. The phase diagram for this system is extensively investigated using a combination of XRD and DTA [38,51–55]. Mao et al. [38] studied this system using different techniques such as EPMA, XRD, and DSC. They described β phase as orderly stacked units of Bi and Bi_2Te_3 with a large

composition range at low temperature and Bi_2Te and Bi_4Te_3 stable in narrow temperature range in the mushy zone.

The homogeneity range of the Bi_2Te_3 phase was determined by Brebrick [51] by measuring the partial pressure of Te_2 over pre-annealed Bi-Te samples with composition between 59.7-60.2 at. % of Te. Small solubility range may affect the semiconducting property; therefore, the range is important from the view of the thermoelectric property of the material. $\Delta H^{f}_{298.15\,K}$ of Bi_2Te_3 was reported in the range 78-84 kJ/mol by [56–59] by means of calorimetry and vapor pressure measurements. In the previous optimization, Gierlotka et al. [29] used $\Delta H^{f}_{298.15\,K}$ of Bi_2Te_3 as 95.4 kJ/mole which was 10 kJ/mol higher than reported maximum experimental value. Calculated value of $\Delta H^{f}_{298.15\,K}$ of Bi_2Te_3 in present optimization is 85.7 kJ/mol which is in good agreement with the reported values [56–59] within the experimental error range. The mixing enthalpy of the liquid phase was measured by many authors [60–62] using calorimetry. These reported data are consistent with each other and show minimum value at near X_{Te} = 0.55. Mixing enthalpy of liquid measured by Blachnik and Enninga [62] who employed iron calorimetry were slightly higher than the Maekawa et al.[60] and Morgant et al.[61]. Maekawa et al.[60] and Morgant et al.[61]'s data were consistent with each other, therefore, their data were considered for the optimization. The activity of Te in Bi-Te liquid alloys was determined using vapor pressure measurements [63], using Knudsen effusion method [64], and EMF method [65–67]. In addition, the heat capacity of the liquid phase at eutectic composition was measured by Schmid and Sommer [68].

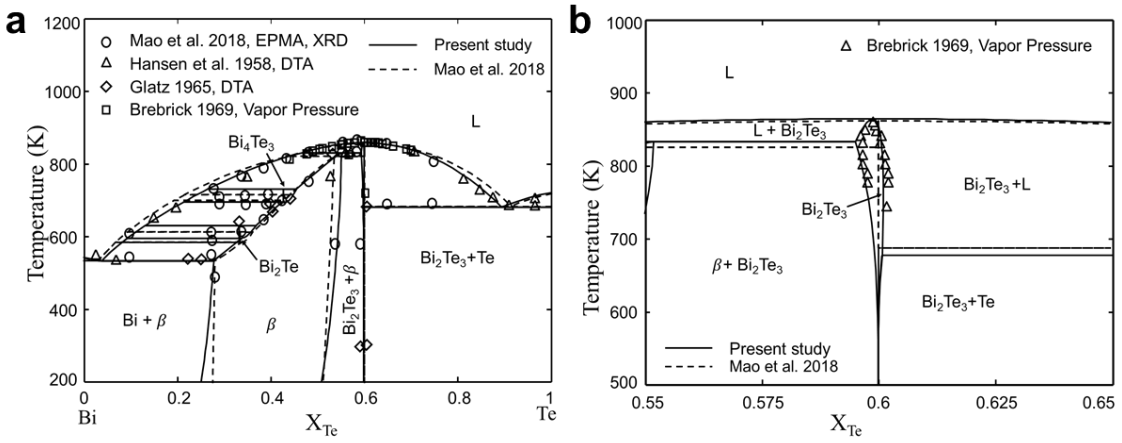

Figure 3 (a) Calculated phase diagram of the Bi-Te system by this work and Mao et al. [38] *and (b) enlarged homogeneity range of Bi_2Te_3 along with experimental data* [38,51,53,54]

In the present study, the liquid phase was modeled using MQM. The Gibbs energy description of the solid phases Bi_2Te, Bi_4Te_3, Bi_2Te_3, and solid solution β phase were adopted from previous optimization [29], however, some modifications such as the enthalpy and entropy of formation at 298.15 K for the solid phases were made to fit the phase diagram and thermodynamic data. The parameter of β phase has been changed to fix the liquidus curve on Bi-rich side. Only one interaction parameter was sufficient to describe the phase β, whereas two parameters were used in the previous optimization [29]. Calculated phase diagram and enlarged high temperature homogeneity range of the Bi_2Te_3 phase along with experimental data [38,51,53,54] are shown in the figure 3(a) and 3 (b), respectively. The calculated phase diagram is in good agreement with the experimental data. The calculated activity of Bi(l) and Te(l) in the liquid and mixing enthalpy of the liquid are shown in figure 4 (a) and 4 (b), respectively. The calculated activity of Bi and Te in the liquid phase agrees well with the experimental data [63–67] and one by Mao et al.[38]. Calculated mixing enthalpy of the liquid phase is in good agreement with experimental data [60,61] except for the mixing enthalpy data [62], which was

slightly higher than those reported in [60,61]. However, Gierlotka et al. [29] put more weight on the higher data by Blachnik & Enninga [62]. Since Blachnik & Enninga [62]'s data showed asymmetry with the minimum value at X_{Te} = 0.6, Gierlotka et al. [29] added an associate of Bi_2Te_3 with complex parameters to reproduce it. On the other hand, the present study and the previous optimization by Mao et al. [38] have considered the liquid solution symmetry in the binary Bi-Te system.

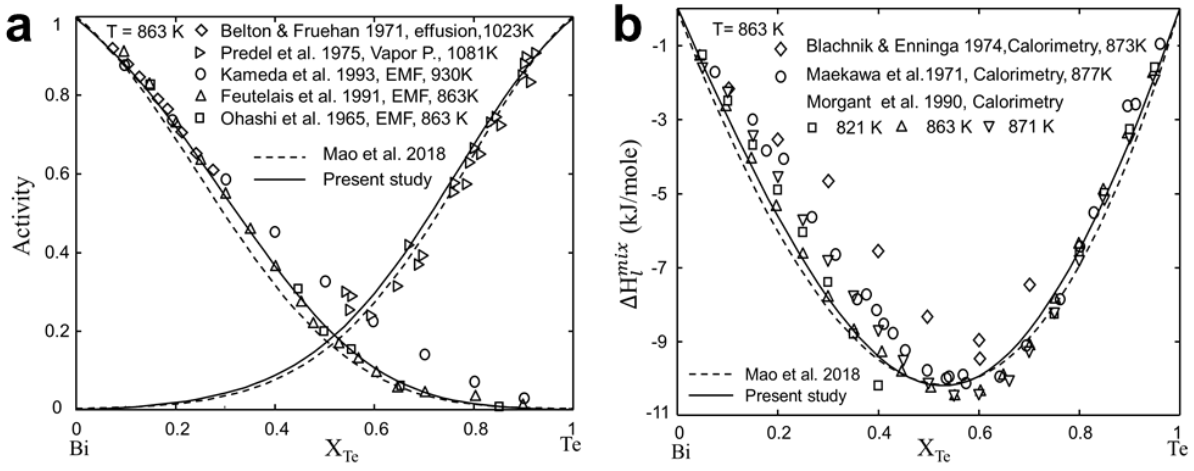

Figure 4 (a) Calculated activity of Bi(l) and Te(l) at 1081 and 863 K along with experimental data [63–67] *and (b) mixing enthalpy of liquid Bi-Te solution at 863 K along with experimental data* [60–62] *and calculation by Mao et al.* [38].

3.4 Ga-Te binary system

Previously, this system has been optimized by Irle et al.[69], Oh and Lee [70] and Liu et al. [71]. Irle et al. [69] used the associate solution model with Ga_2Te_3 as an associate component, while Oh and Lee [70] and Liu et al. [71] used the ionic model for liquid solution. The only difference between Oh and Lee [70] and Liu et al. [71] is that the latter used the latest lattice stability parameter of Te and revised the phase diagram by slight modification in model parameters. They have extensively reviewed the available thermodynamic data and those data

were employed in the present study to determine the model parameter for this system. Klemm and Vogel [72] reported phase diagram data in the Ga-Te system using thermal and qualitative X-Ray analysis and identified the two compounds GaTe and Ga_2Te_3. Dale [73] reported GaTe and Ga_2Te_3 using metallographic investigation and hardness measurement in the composition range 50-80 at. % Te. Alapini et al. [74] investigated the phase diagram using DTA and X-ray diffraction studies and reported Ga_2Te_5 compound in the temperature ranges 673-768 K together with those reported by Klemm and Vogel [72] GaTe and Ga_2Te_3. Antonopoulo et al.[75] reported another compound Ga_3Te_4 based on a study by electron microscope. Tschirner et al. [76] investigated tellurium-rich side of the phase diagram using differential thermal analysis and confirmed the four previously reported compounds GaTe, Ga_2Te_3, Ga_3Te_4, and Ga_2Te_5. These four compounds were also confirmed by Blachnik and Irle [77] using DTA. Glazov and Pavlova [78] determined the liquidus curve at composition range 40-70 at. % Te through thermal analysis. M. Wobst [79] investigated the Ga-rich miscibility gap by thermal analysis. Recently, the liquidus curve was reported by Mouani et al. [80] by means of DTA, DSC, X-ray powder diffraction, and metallographic analysis. The calculated phase diagram is shown in figure 5 along with experimental data [72,74,76,78–80] and previous calculation [71].

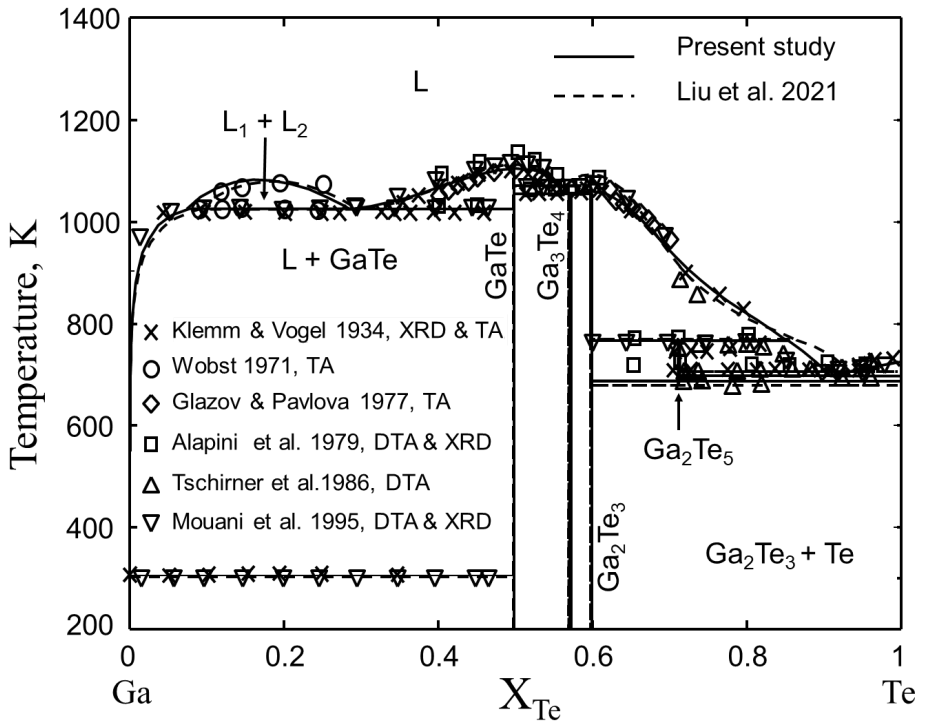

Figure 5 Calculated phase diagram of binary Ga-Te system along with experimental data [72,74,76,78–80] *and previous calculation* [71].

The activity in liquid solution was reported using vapor pressure [81,82] and EMF method [83,84]. The mixing enthalpy of the liquid solution was measured using calorimetry analysis [69,85–87]. Moreover, partial enthalpy of Te and Ga in the liquid solution was determined using calorimetry [69] and vapor pressure measurements [81]. Mixing enthalpy of liquid phase show a sharp minimum around 60 at. % Te because of SRO in the liquid phase. Considering the SRO in liquid phase, the solution was optimized using MQM. The calculated activity of Ga(l) and Te(l) in liquid is shown in figure 6 (a) along with experimental data [81–84]. Calculated integral and partial enthalpy of mixing of Ga(l) and Te(l) in the liquid are shown in figure 6 (b) and 6 (c), respectively, along with the experimental data [69,81,85–87] and previous calculation [71]. The calculated thermodynamic properties of the liquid phase agree well with the experimental data.

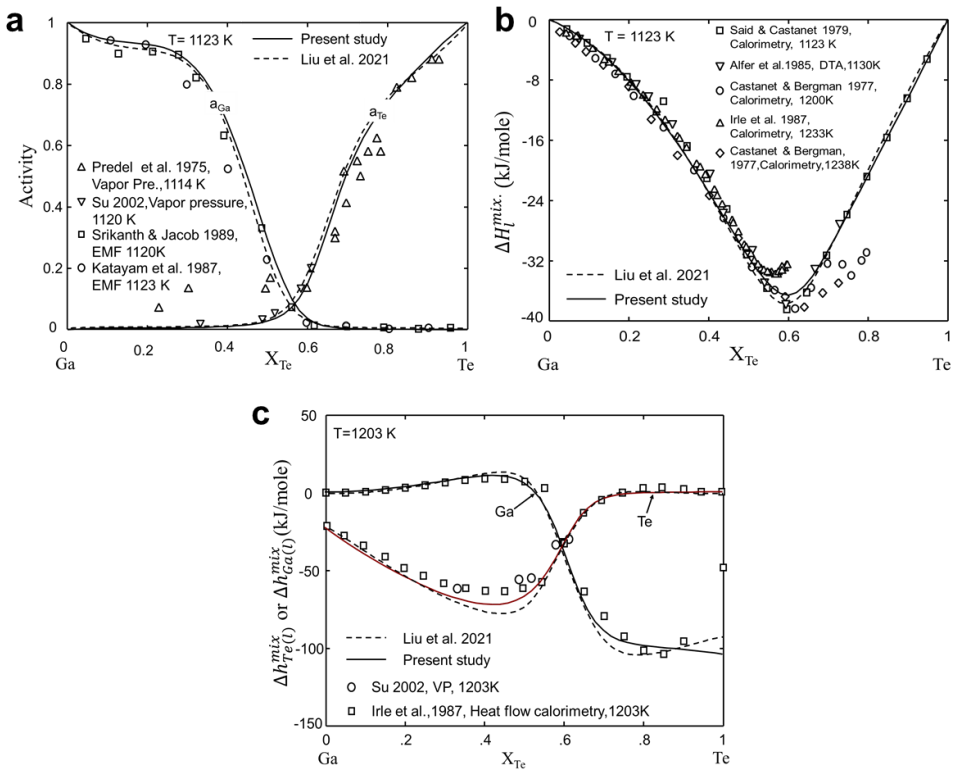

Figure 6 (a) Calculated activity of Ga(l) and Te(l) in liquid at 1123 K along with experimental data [81–84]*, (b) mixing enthalpy of liquid at 1123 K along with experimental data* [69,85–87] *and (c) partial mixing enthalpy of Ga(l) and Te(l) in liquid at 1203 K along with experimental data* [69,81] *and calculation by Liu et al.* [71].

In previous optimizations, Oh and Lee [70] used a constant heat capacity function and Liu et al. [71] estimated the function from the reference state of the constituent elements for example $C_p^{GaTe} = C_p^{Ga} + C_p^{Te}$ for intermetallic compounds in this system. The heat capacity of GaTe is measured by Pashinkin et al.[32] using DSC, and by Sedmidubský et al. [31] using DSC and temperature relaxation method in the temperature range of 350-600 K. Tyurin et al. [30] measured heat capacity of GaTe and Ga_2Te_3 in the temperature range 6.8 to 337.95 K using adiabatic calorimetry. These measured heat capacity values are much different than the heat capacity function used in the previous optimization [70,71]. Therefore, the heat capacity functions for the compound GaTe and Ga_2Te_3 were reassessed and the calculated results are

shown in figure 7 (a), and 7 (b) along with experimental data [30–32] and previously calculated heat capacity [70,71]. There was no measured heat capacity available for the compounds Ga_3Te_4 and Ga_2Te_5. Therefore, the following heat capacity functions were used for the one mole of Ga_3Te_4 and Ga_2Te_5:

$$C_p^{Ga3Te4} = C_p^{Ga2Te3} + C_p^{GaTe} \quad (15)$$

$$C_p^{Ga2Te5} = 2C_p^{Ga} + 5C_p^{Te} \quad (16)$$

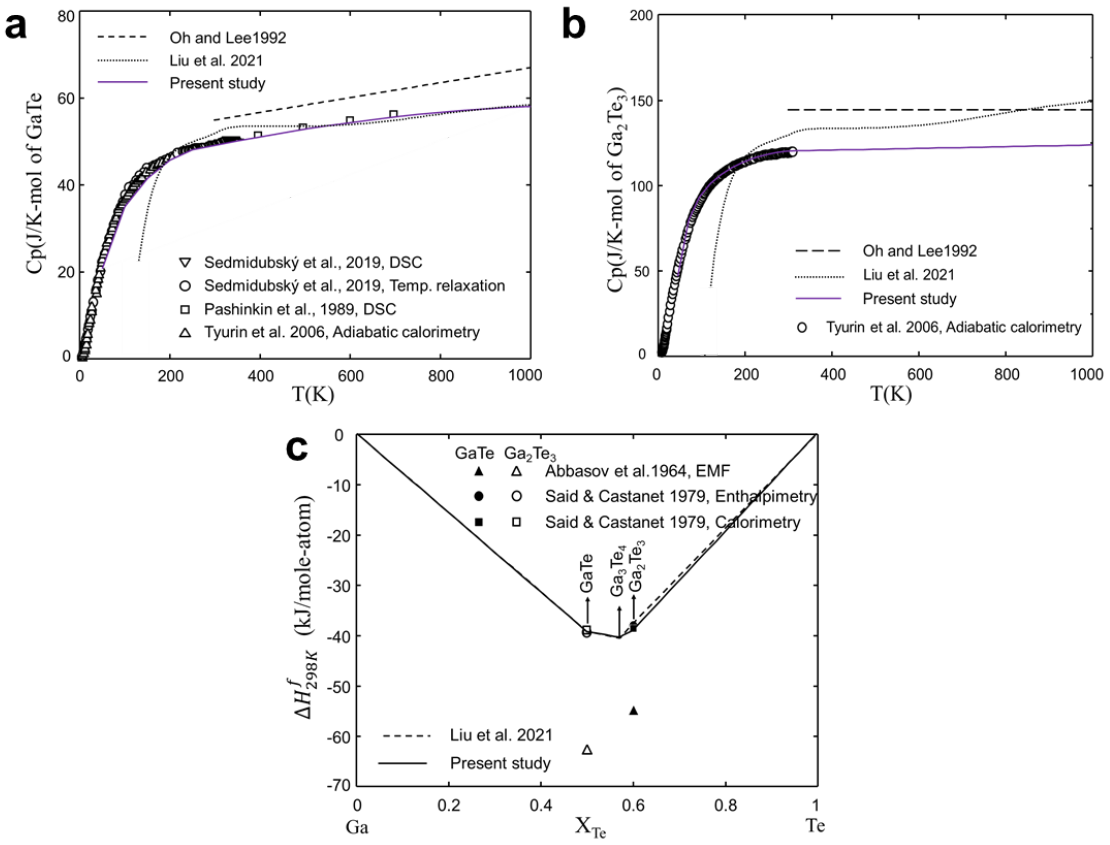

Figure 7 Calculated heat capacity of (a) GaTe (b) Ga_2Te_3 along with respective experimental data [30–32] *and (c) formation enthalpy at 298.15 K along with experimental data* [86,88] *and calculated by* [70,71].

$\Delta H^{f}_{298.15K}$ of intermetallic compounds, GaTe and Ga_2Te_3 are determined by Abbasov et al. [88] using the EMF method. Said and Castanet [86] measured the formation enthalpy of GaTe and Ga_2Te_3 at 298.15 K using Enthalpimetry and dissolution calorimetry. Abbasov et al. [88]'s data were around 20 kJ lower in comparison to the Said and Castanet [86]. Since calorimetrically measured enthalpy is more reliable than EMF. Therefore, Said and Castanet's [86] data were preferred in the present study. No thermochemical information was available for the compounds Ga_3Te_4 and Ga_2Te_5, therefore, $\Delta H^{f}_{298.15K}$ and $S_{298.15\,K}$ were fixed by fitting phase diagram data. The calculated enthalpy of formation at 298.15 K is shown in figure 7 (c) along with experimental data [86,88] and calculated by [70,71].

3.4 Ga-Bi-Te ternary system

Rustamov et al. [89,90] investigated the physiochemical interaction along four internal sections of the ternary Bi-Ga-Te system: Bi-GaTe, Bi-Ga_2Te_3, Bi_2Te_3-GaTe, and Bi_2Te_3-Ga. The alloy compositions along these sections were equilibrated at 400 ℃ for 500 hrs. and investigated using DTA, microstructural examination, and micro-hardness measurements. Based on the investigations, 17 curves of univariant equilibrium that divide the liquidus into 10 primary crystallization fields of the phases i.e., Te, Be, Ga_3Te_2, GaTe, Ga_2Te_3, $GaTe_3$, Bi_2Te_3, BiTe, Bi_2Te, and $Bi_{14}Te_6$ were reported. Based upon the available internal sections and liquidus projection in the literature, Shakhbazov et al. [91] reported the isothermal sections at 600, 400, and 200 ˚C of the system. There is no ternary compound phase reported in this system.

Reported quasi binary Bi_2Te_3-GaTe forms a eutectic at composition 65 mole % of Bi_2Te_3 at 823 K, whereas eutectic in quasi binary Bi-GaTe is formed at 97 mole % and 513 K.

In the present study, "Toop-like" asymmetric approximation [37] with Te as an asymmetric component was used as a first approximation of Gibbs free energy of the ternary liquid solution in the Bi-Ga-Te system. No ternary parameter is added in the system and the calculations in the ternary system are only predictions from the binary systems. The calculated sections: GaTe-Bi, Ga_2Te_3-Bi_2Te_3, GaTe- Bi_2Te_3, Ga_2Te_3-Bi, and Bi_2Te_3-Ga are shown in figure 8 (a-f) respectively, along with experimental data by Rustamov et al. [89,90]. As seen in figure 8(a), the calculated liquidus temperature is higher in the Bi rich region compared to experimental data. This could be due to the metastable liquid miscibility gap (dotted line in figure 8(a) below the liquidus line. Similarly, at the Bi-rich side in figure 8 (c) and Ga-rich side in figure 8 (e), the calculated liquidus is slightly higher than the experimental data. In order to fix the liquidus line in these sections, a large negative ternary parameter should be added on Bi rich side. However, this was not done for two reasons. Firstly, the liquidus temperature and the eutectic composition in the in Ga_2Te_3-Bi_2Te_3 section (see Fig. 8 (b)) and Ga_2Te_3-Bi section (see Fig. 8 (d) is accurately predicted without any addition of ternary parameters. In addition, the eutectic compositions and temperature range in the rest of the sections are reasonably predicted as well. Since the objective of this work is to suggest eutectic compositions for TE applications, the calculations in the ternary system can fulfill this objective without the necessity of adding any ternary parameter. Secondly, in future, the present database will be combined with Sn-Ga-Te and In-Ga-Te systems to suggest multiphase eutectic microstructures for TE applications. Therefore, for reasonable predictions in the multicomponent Sn-Ga-Te-Bi system, it is best to use none or minimum number of ternary parameters.

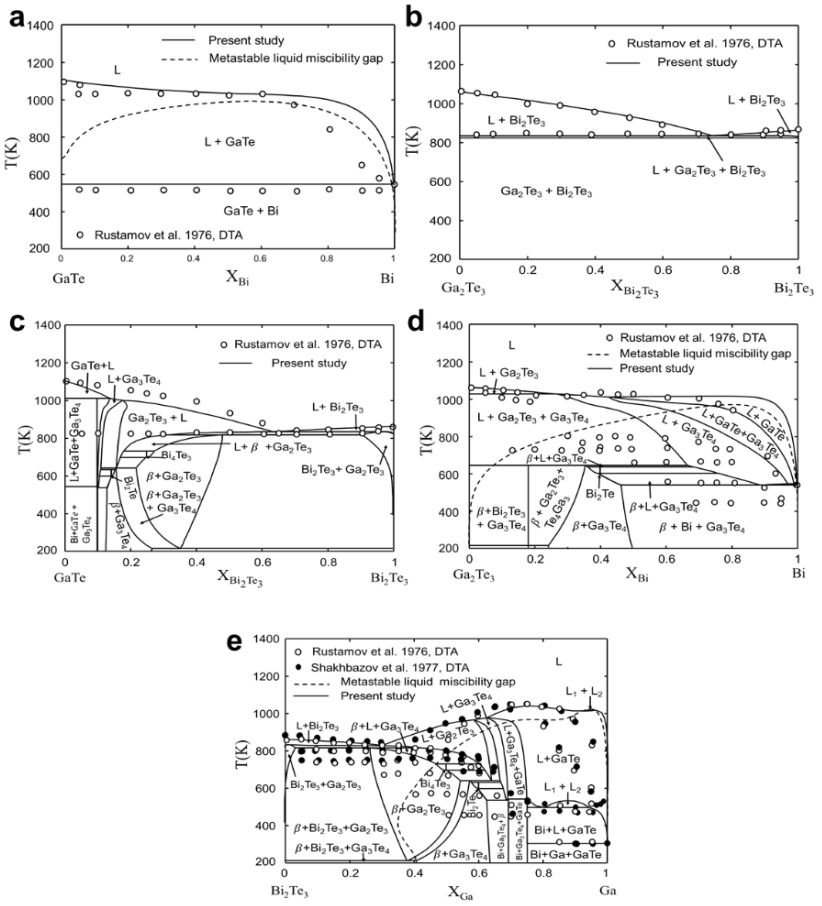

Figure 8 Calculated vertical section of (a) the GaTe-Bi (b) Ga_2Te_3-Bi_2Te_3 (c) GaTe-Bi_2Te_3 (d) Ga_2Te_3-Bi (e) Bi_2Te_3-Ga quasi-binaries along with experimental data [89,90].

The calculated liquidus projection over the entire composition range of the system Ga-Bi-Te is shown in figure 9. The points located at the intersections of the solid lines correspond to invariant equilibria. The different types of invariant reactions, their compositions, and temperatures are listed in table 2.

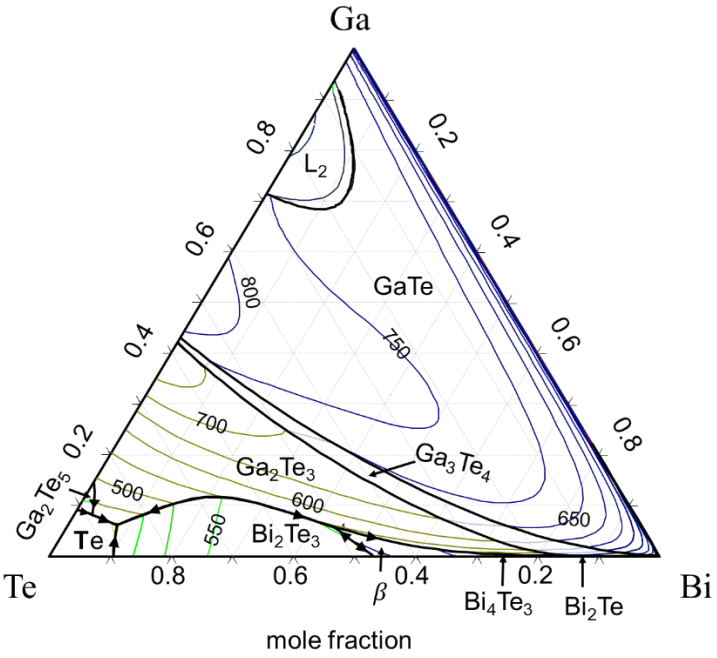

Figure 9 Calculated liquidus projection in the Ga-Bi-Te system

Table 2 Invariant reactions in Ga-Bi-Te system

	Reaction	Type	Composition			T (K)
			X_{Bi}	X_{Ga}	X_{Te}	
1	$L + Bi_2Te_3 \leftrightarrow \beta + Ga_2Te_3$	QP	0.439	0.057	0.504	816.75
2	$L + \beta + Ga_2Te_3 \leftrightarrow Bi_4Te_3$	P	0.727	3.4E-3	0.269	729.49
3	$L + Bi_2Te \leftrightarrow \beta + Ga_3Te_4$	QP	0.867	3.0E-4	0.132	728.38
4	$L + Bi_4Te_3 \leftrightarrow \beta + Ga_2Te_3$	P	0.782	1.3E-3	0.217	695.83

5	$L + Ga_2Te_5 \leftrightarrow Te + Ga_2Te_3$	QP	0.03	0.08	0.89	686.36
6	$L \leftrightarrow Bi_2Te_3 + Te + Ga_2Te_3$	E	0.08	0.06	0.86	667.94
7	$L + Ga_2Te_3 \leftrightarrow \beta + Ga_3Te_4$	QP	0.856	4.0E-4	0.144	640.82
8	$L + Bi_2Te \leftrightarrow Ga_3Te_4 + \beta$	P	0.905	1.5E-4	0.094	596.93
9	$L + GaTe \leftrightarrow Bi + Ga_3Te_4$	QP	0.988	6.0E-4	0.011	542
10	$L \leftrightarrow \beta + Bi + Ga_3Te_4$	E	0.959	7.0E-5	0.404	534.71

P: Peritectic, E: Eutectic, QP: Quasi Peritectic.

4. Application of the database

Based on the present calculations, four sections in the Ga-Bi-Te system that can be of great potential to be used in TE application are shown in Fig. 10 (a-d), respectively. The prospective compositions are marked using red circle in the figure 10. For example, cooling of marked composition in figure 10 (b) involves eutectic reaction $L \leftrightarrow Ga_2Te_3 + Bi_2Te_3$. A previous study reported improved TE properties of Bi_2Te_3-In_2Te_3 eutectic alloys [22]. Ga_2Te_3 exhibits a similar crystal structure as In_2Te_3 and has promising thermoelectric properties [92], hence eutectic of Ga_2Te_3-Bi_2Te_3 could be a great potential to be used as a TE alloy. Further, various other compositions shown in Fig. 10 can be explored for TE application and the influence of

microstructures features such as lamellar spacing, eutectic size, crystallographic orientation can be co-related with the TE properties.

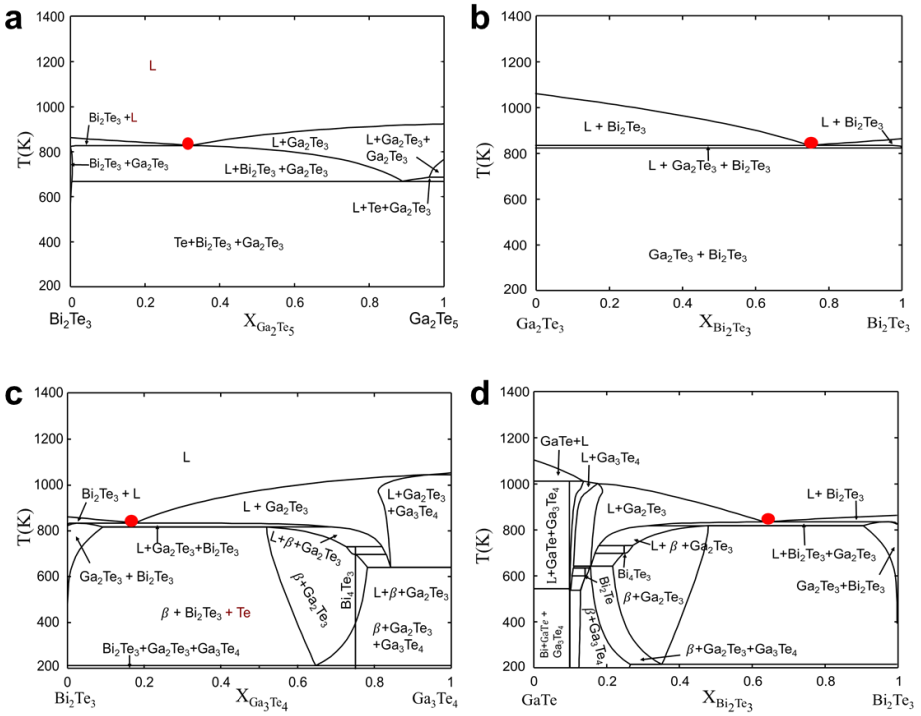

Figure 10 Calculated vertical sections of (a) the Bi_2Te_3-Ga_2Te_5 (b) Ga_2Te_3-Bi_2Te_3 (c) Bi_2Te_3-Ga_3Te_4 (d) GaTe-Bi_2Te_3 quasi-binaries.

4 Conclusions

In this study, Ga-Bi-Te and related sub binaries are thermodynamically assessed based on available experimental information using the CALPHAD method. The liquid solution in binary Ga-Te, Bi-Te, and Bi-Ga system was reassessed by using the Modified Quasichemical Model (MQM) to account for the short-range ordering (SRO) exhibited by the liquid solution. Solid phases GaTe, Ga_3Te_4. Ga_2Te_3 and Ga_2Te_5 in Ga-Te binary system; Bi_2Te and Bi_4Te_3 in Bi-Te binary system were considered as line compound; solid solutions β and Bi_2Te_3 in Bi-Te were modeled using Compound Energy Formalism. A set of self-consistent thermodynamic

description was obtained for all the phases in the Ga-Bi, Bi-Te, and Ga-Te binary systems. The available thermodynamic and phase diagram data were reproduced within the experimental error range. Combining the optimized sub-binary systems, thermodynamic properties of the ternary Bi-Ga-Te were predicted reasonably well without any additional ternary model parameter. Several ternary eutectic compositions for Thermoelectric applications are predicted from the current database. Further, the optimized database will be extended to a larger telluride-based system by adding elements such as In, Sn to explore the multiphase eutectic systems for thermoelectric (TE) applications.

Data Availability Statement

The raw data required to reproduce these findings are available to download from the online submission system and is included in the folder “Data in Brief “

5 References:

[1] G.J. Snyder, E.S. Toberer, Complex thermoelectric materials, Nat. Mater. 7 (2008) 105–114. https://doi.org/10.1038/nmat2090.

[2] L.E. Bell, Cooling, heating, generating power, and recovering waste heat with thermoelectric systems, Science (80-.). 321 (2008) 1457–1461. https://doi.org/10.1126/science.1158899.

[3] G.S. Nolas, J. Poon, M. Kanatzidis, Recent developments in bulk thermoelectric materials, MRS Bull. 31 (2006) 199–205. https://doi.org/10.1557/mrs2006.45.

[4] K. Uchida, S. Takahashi, K. Harii, J. Ieda, W. Koshibae, K. Ando, S. Maekawa, E. Saitoh, Observation of the spin Seebeck effect, Nature. 455 (2008) 778–781. https://doi.org/10.1038/nature07321.

[5] M. Cutler, J.F. Leavy, R.L. Fitzpatrick, Electronic transport in semimetallic cerium sulfide, Phys. Rev. 133 (1964) A1143. https://doi.org/10.1103/PhysRev.133.A1143.

[6] M.N. Hasan, H. Wahid, N. Nayan, M.S. Mohamed Ali, Inorganic thermoelectric materials: A review, Int. J. Energy Res. 44 (2020) 6170–6222. https://doi.org/10.1002/er.5313.

[7] M.G. Kanatzidis, Nanostructured Thermoelectrics: The New Paradigm? †, Chem. Mater. 22 (2010) 648–659. https://doi.org/10.1021/cm902195j.

[8] T.C. Harman, M.P. Walsh, B.E. Laforge, G.W. Turner, Nanostructured Thermoelectric Materials, J. Electron. Mater. 34 (2005) L19–L22. https://doi.org/10.1007/s11664-005-0083-8.

[9] M. Durman, S. Murphy, Precipitation of metastable ϵ-phase in a hypereutectic zinc-aluminium alloy containing copper, Acta Metall. Mater. 39 (1991) 2235–2242. https://doi.org/10.1016/0956-7151(91)90005-L.

[10] J.E. Spinelli, B.L. Silva, A. Garcia, Microstructure, phases morphologies and hardness of a Bi-Ag eutectic alloy for high temperature soldering applications, Mater. Des. 58 (2014) 482–490. https://doi.org/10.1016/j.matdes.2014.02.026.

[11] X.F. Wu, K.Y. Wang, F.F. Wu, R. Da Zhao, M.H. Chen, J. Xiang, S.N. Ma, Y. Zhang, Simultaneous grain refinement and eutectic Mg2Si modification in hypoeutectic Al-11Mg2Si alloys by Sc addition, J. Alloys Compd. 791 (2019) 402–410. https://doi.org/10.1016/j.jallcom.2019.03.326.

[12] P. Blanco-Rodríguez, J. Rodríguez-Aseguinolaza, E. Risueño, M. Tello, Thermophysical characterization of Mg-51%Zn eutectic metal alloy: A phase change material for thermal energy storage in direct steam generation applications, Energy. 72 (2014) 414–420. https://doi.org/10.1016/j.energy.2014.05.058.

[13] S.L. Li, J.M. Song, J.Y. Uan, Mg-Mg2X (X=Cu, Sn) eutectic alloy for the Mg2X

nano-lamellar compounds to catalyze hydrolysis reaction for H2 generation and the recycling of pure X metals from the reaction wastes, J. Alloys Compd. 772 (2019) 489–498. https://doi.org/10.1016/j.jallcom.2018.09.154.

[14] T. Ikeda, E.S. Toberer, V.A. Ravi, S.M. Haile, G. Jeffrey Snyder, Lattice thermal conductivity of self-assembled PbTe-Sb2Te 3 composites with nanometer lamellae, in: Int. Conf. Thermoelectr. ICT, Proc., 2007: pp. 1–4. https://doi.org/10.1109/ICT.2007.4569408.

[15] J.-H. Yim, K. Jung, H.-J. Kim, H.-H. Park, C. Park, J.-S. Kim, Effect of Composition on Thermoelectric Properties in PbTe-Bi2Te3 Composites, J. Electron. Mater. 40 (2011) 1010–1014. https://doi.org/10.1007/s11664-010-1485-9.

[16] J.R. Sootsman, J. He, V.P. Dravid, S. Ballikaya, D. Vermeulen, C. Uher, M.G. Kanatzidis, Microstructure and Thermoelectric Properties of Mechanically Robust PbTe-Si Eutectic Composites , Chem. Mater. 22 (2010) 869–875. https://doi.org/10.1021/cm9016672.

[17] J. Dadda, E. Müller, S. Perlt, T. Höche, R. Hermann, A. Neubrand, Evolution of phase segregation and eutectic structures in AgPb18SbTe20, Phys. Status Solidi. 211 (2014) 1276–1281. https://doi.org/10.1002/pssa.201300199.

[18] H.J. Wu, W.J. Foo, S.W. Chen, G. Jeffrey Snyder, Ternary eutectic growth of nanostructured thermoelectric Ag-Pb-Te materials, Appl. Phys. Lett. 101 (2012) 023107. https://doi.org/10.1063/1.4733661.

[19] O.E. Femi, K. Akkiraju, B.S. Murthy, N. Ravishankar, K. Chattopadhyay, Effect of processing route on the bipolar contribution to the thermoelectric properties of n-type eutectic Bi22.5Sb7.5Te70 alloy, J. Alloys Compd. 682 (2016) 791–798. https://doi.org/10.1016/j.jallcom.2016.05.054.

[20] J.Q. Li, L.F. Li, S.H. Song, F.S. Liu, W.Q. Ao, High thermoelectric performance of GeTe-Ag8GeTe6 eutectic composites, J. Alloys Compd. 565 (2013) 144–147. https://doi.org/10.1016/j.jallcom.2013.02.149.

[21] Y. Cheng, J. Yang, Q. Jiang, D. He, J. He, Y. Luo, D. Zhang, Z. Zhou, Y. Ren, J. Xin, New insight into InSb-based thermoelectric materials: from a divorced eutectic design to a remarkably high thermoelectric performance, J. Mater. Chem. A. 5 (2017) 5163–5170. https://doi.org/10.1039/c6ta10827j.

[22] D. Liu, C. Dreβler, M. Seyring, S. Teichert, M. Rettenmayr, Reduced thermal conductivity of Bi-In-Te thermoelectric alloys in a eutectic lamellar structure, J. Alloys Compd. 748 (2018) 730–736. https://doi.org/10.1016/j.jallcom.2018.03.201.

[23] B. Yang, S. Li, X. Li, Y. Wang, H. Zhong, S. Feng, Microstructure and enhanced thermoelectric performance of Te–SnTe eutectic composites with self-assembled rod and lamellar morphology, Intermetallics. 112 (2019) 106499. https://doi.org/10.1016/j.intermet.2019.106499.

[24] X. Tang, W. Xie, H. Li, W. Zhao, Q. Zhang, M. Niino, Preparation and thermoelectric transport properties of high-performance p-type Bi2Te3 with layered nanostructure,

Appl. Phys. Lett. 90 (2007) 012102. https://doi.org/10.1063/1.2425007.

[25] C. Lin, W. Yen, Y. Tsai, H. Wu, Unraveling p-n Conduction Transition in High Thermoelectric Figure of Merit Ga-doped Bi2Te3 via Phase Diagram Engineering, ACS Appl. Energy Mater. 3 (2020) 1311–1318. https://doi.org/10.1021/acsaem.9b02500.

[26] A.D. Pelton, S.A. Degterov, G. Eriksson, C. Robelin, Y. Dessureault, The modified quasichemical model I—Binary solutions, Metall. Mater. Trans. B. 31 (2000) 651–659. https://doi.org/10.1007/s11663-000-0103-2.

[27] A.D. Pelton, and P. Chartrand, The Modified Quasi-chemical Model: Part II. Multicomponent Solutions, Met. Mater. Trans. A,. 32(6) (2001) 1355–1360. https://doi.org/10.1007/s11661-001-0226-3.

[28] M. Hillert, The compound energy formalism, J. Alloys Compd. 320 (2001) 161–176. https://doi.org/10.1016/S0925-8388(00)01481-X.

[29] W. Gierlotka, A new thermodynamic description of the binary Bi-Te system using the associate solution and the Wagner-Schottky models, Calphad Comput. Coupling Phase Diagrams Thermochem. 63 (2018) 6–11. https://doi.org/10.1016/j.calphad.2018.08.005.

[30] A. V Tyurin, K.S. Gavrichev, V.P. Zlomanov, N.N. Smirnova, Low-Temperature Heat Capacity and Thermodynamic Functions of GaTe, Neorg. Mater. 42 (2006) 945–948. https://doi.org/10.1134/S0020168506080097.

[31] D. Sedmidubský, Z. Sofer, Š. Huber, J. Luxa, R. Točík, T. Mahnel, K. Růžička, Chemical bonding and thermodynamic properties of gallium and indium monochalcogenides, J. Chem. Thermodyn. 128 (2019) 97–102. https://doi.org/10.1016/j.jct.2018.08.013.

[32] A.S. Pashinkin, A.S. Malkova, V.V. Zharov, Specific heat of gallium and indium monotellurides, Zhurnal Fiz. Khimii. 63 (1989) 1621–1623. https://inis.iaea.org/search/search.aspx?orig_q=RN:21082578.

[33] C.W. Bale, P. Chartrand, S.A. Degterov, G. Eriksson, K. Hack, R. Ben Mahfoud, J. Melançon, A.D. Pelton, S. Petersen, FactSage thermochemical software and databases, Calphad Comput. Coupling Phase Diagrams Thermochem. 26 (2002) 189–228. https://doi.org/10.1016/S0364-5916(02)00035-4.

[34] C.W. Bale, E. Bélisle, P. Chartrand, S.A. Decterov, G. Eriksson, K. Hack, I.H. Jung, Y.B. Kang, J. Melançon, A.D. Pelton, C. Robelin, S. Petersen, FactSage thermochemical software and databases - recent developments, Calphad Comput. Coupling Phase Diagrams Thermochem. 33 (2009) 295–311. https://doi.org/10.1016/j.calphad.2008.09.009.

[35] A.T. Dinsdale, SGTE Data for Pure Elements, Calphad. 15 (1991) 317–425.

[36] H. Kopp, Investigations of the Specific Heat of Solid Bodies, Philos. Trans. Roy. Sot. London. 155 (1865) 71–202. https://doi.org/10.1098/rstl.1865.0003.

[37] A.D. General, and A. Pelton, A general “geometric” thermodynamic model for multicomponent solutions, Calphad. 25 (2001) 319–328.

https://doi.org/10.1016/S0364-5916(01)00052-9.

[38] C. Mao, M. Tan, L. Zhang, D. Wu, W. Bai, L. Liu, Experimental reinvestigation and thermodynamic description of Bi-Te binary system, Calphad Comput. Coupling Phase Diagrams Thermochem. 60 (2018) 81–89. https://doi.org/10.1016/j.calphad.2017.11.007.

[39] C. Girard, R. Baret, J. Riou, J.M. Miane, J.P. Bros, Thermodynamic study of the Al-Bi-Ga system by potentiometry and D.T.A., Fluid Phase Equilib. 20 (1985) 331–339. https://doi.org/10.1016/0378-3812(85)90052-4.

[40] N.A. Puschin, S. Stepanović, V. Stajić, Über die Legierungen des Galliums mit Zink, Cadmium, Quecksilber, Zinn, Blei, Wismut und Aluminium, Zeitschrift Für Anorg. Und Allg. Chemie. 209 (1932) 329–334. https://doi.org/10.1002/zaac.19322090318.

[41] B. Predel, Die Zustandsbilder Gallium-Wismut und Gallium-Quecksilber, Vergleich der Koexistenzkurven mit den Theorien der Entmischung, Zeitschrift Fur Phys. Chemie. 24 (1960) 206–216. https://doi.org/10.1524/zpch.1960.24.3_4.206.

[42] B. Huber, K.W. Richter, H. Flandorfer, A. Mikula, H. Ipser, Thermodynamic characterization of liquid alloys with demixing tendency: Bi-Ga, Zeitschrift Fuer Met. Res. Adv. Tech. 99 (2008) 18–23. https://doi.org/10.3139/146.101601.

[43] A.S. Jordan, Calculation of phase equilibria in the Ga-Bi and Ga-P-Bi systems based on a theory of regular associated solutions, Metall. Trans. B. 7 (1976) 191–202. https://doi.org/10.1007/BF02654917.

[44] D. Manasijević, D. Minić, D. Živković, I. Katayama, J. Vřešťál, D. Petković, Experimental investigation and thermodynamic calculation of the Bi-Ga-Sn phase equilibria, J. Phys. Chem. Solids. 70 (2009) 1267–1273. https://doi.org/10.1016/j.jpcs.2009.07.010.

[45] B. Predel, M. Frebel, W. Gust, Untersuchung Der Thermodynamisches Eigenschaften Flussiger Gallium-Zinn Und Gallium-wismut-Legierungen, J. Less Common Met. 17 (1969) 391–402. https://doi.org/10.1016/0022-5088(69)90065-4.

[46] S. Yatsenko, V.N. Danilin, No Title, Izv. Akad. Nauk SSSR, Neorg. Mater. 4 (1968) 863–867.

[47] I. Katayama, J. Nakayama, T. Ikura, Z. Kozuka, T. Lida, Activity Measurement of Gallium in Ga–Bi and Ga–Sb–Bi Alloys by EMF Method Using Zirconia as Solid Electrolyte, Mater. Trans. 34 (1993) 792–795. https://www.jstage.jst.go.jp/article/matertrans1989/34/9/34_9_792/_article/-char/ja/.

[48] M. Gambino, J.P. Bros, F. Ajersch, I. Ansara, Contribution à l'étude thermodynamique du système bismuth-gallium, Thermochim. Acta. 14 (1976) 305–313. https://doi.org/10.1016/0040-6031(76)85007-1.

[49] Z. MOSER, K. RZYMAN, Calorimetric studies on Bi-Ga liquid alloys, Arch. Hut. 32 (1987) 3–8. http://pascal-francis.inist.fr/vibad/index.php?action=getRecordDetail&idt=7663141.

[50] D. Živković, D. Manasijević, Ž. Živković, Comparative thermodynamic investigation of binary Ga-Bi system: Experimental determination of enthalpies of mixing and activity estimation for liquid Ga-Bi alloys, J. Therm. Anal. Calorim. 79 (2005) 71–77. https://doi.org/10.1007/s10973-004-0564-7.

[51] R.F. Brebrick, Homogeneity ranges and Te2-pressure along the three-phase curves for Bi2Te3(c) and a 55-58 at.% Te, peritectic phase, J. Phys. Chem. Solids. 30 (1969) 719–731. https://doi.org/10.1016/0022-3697(69)90026-2.

[52] A. Brown, B. Lewis, The systems bismuth-tellurium and antimony-tellurium and the synthesis of the minerals hedleyite and wehrlite, J. Phys. Chem. Solids. 23 (1962) 1597–1604. https://doi.org/10.1016/0022-3697(62)90242-1.

[53] A.C. Glatz, An Evaluation of the Bismuth-Tellurium Phase System, J. Electrochem. Soc. 112 (1965) 1204–1207. https://doi.org/10.1149/1.2423400.

[54] M. Hansen, K. Anderko, H.W. Salzberg, Constitution of binary alloys, J. Electrochem. Soc. 105 (1958) 260–261. https://www.scopus.com/record/display.uri?eid=2-s2.0-65449122493&origin=inward.

[55] V. Glazov, L. Pavlova, Y. Yatmanov, A Thermodynamic Assessment and Experimental Verification of the Possibility of Diffusionless Crystallisation of Alloys in the Bi-Te System, Russ. J. Phys. Chem. 58 (1984) 176–180.

[56] B.W. Howlett, S. Misra, M.B. Bever, On the Thermodynamic Properties of the Compounds Sb2Se3, Bi2Se3, Sb2Te3, and Bi2Te3, Trans. Met. Soc. AIME. 230 (1964) 1367–1372.

[57] Z. Boncheva-Mladenova, A.S. Pashinkin, A. V. Novoselova, Investigation of the Evaporation of Antimony and Bismuth Tellurides and of Bismuth Selenide, Neorg. Chem. Bond. Solids. 3 (1972) 151–158. https://doi.org/10.1007/978-1-4684-1686-2_26.

[58] A.A. Vecher, L.A. Mechkovskii, A.S. Skoropanov, Determination of heats of formation of some tellurides, Izv. Akad. Nauk SSSR, Neorg. Mater. 10 (1974) 2140–2143.

[59] V.R. Sidorko, L. V Goncharuk, R. V Antonenko, THERMODYNAMIC PROPERTIES OF BISMUTH SESQUISELENIDE AND SESQUITELLURIDE AND THEIR SOLID SOLUTIONS, 2008. https://doi.org/10.1007/s11106-008-9009-3.

[60] T. Maekawa, T. Yokokawa, K. Niwa, Enthalpies of mixing in the liquid state. Tl + Te and Bi + Te, J. Chem. Thermodyn. 3 (1971) 143–150. https://doi.org/10.1016/S0021-9614(71)80075-7.

[61] G. Morgant, Y. Feutelais, B. Legendre, R. Castanet, A. Coulet, Themodynamic behaviour of Bi-Te alloys, Z. Met. 81 (1990) 44–48.

[62] R. blachnik, E. Enninga, Mischungsenthalpien im flüissigen BiTe System, Thermochim. Acta. 9 (1974) 83–86. https://doi.org/10.1016/0040-6031(74)85099-9.

[63] B. Predel, J. Piehl, M.J. Pool, Contribution to the thermodynamic properties of liquid binary alloys of Te with Sn, Pb and Bi, Zeitschrift Fuer Met. 66 (1975) 347–352.

http://inis.iaea.org/Search/search.aspx?orig_q=RN:7223361.

[64] G.H. Belton, R.J. Fruehan, The determination of the activities by Mass-Spectrometry-Some Additional Methods, Metall. Trans. 2 (1971) 291–296. https://doi.org/10.1007/BF02662673.

[65] T. Ohashi, Z. Kozuka, J. Moriyama, No Title, Nagoya Kogyo Deigaku Gakuho. 17 (1965) 354–357. Taken from Feutelais et al. 1991.

[66] Y. Feutelais, G. Morgant, B. Legendre, Liquid state electrochemical study of bismuth-tellurium liquid alloys, J. Less-Common Met. 169 (1991) 197–207. https://doi.org/10.1016/0022-5088(91)90068-F.

[67] K. Kameda, K. Yamaguchi, H. Horie, Activity of Liquid Te-Bi alloys measured by an EMF method using Zirconia Electrolyte, J. Japan Inst. Met. 57 (1993) 158–193.

[68] J. Schmid, F. Sommer, Heat capacity of liquid Eutectic Tellurium alloys, Ber. Bunsenges. Phys. Chem. 102 (1998) 1279–1283. https://doi.org/10.1002/bbpc.19981020937.

[69] E. IRLE, B. GATHER, R. BLACHNIK, U. KATTNER, H.L. LUKAS, G. PETZOW, ChemInform Abstract: Enthalpies of Mixing of the Melt and Thermodynamic Optimization of the Gallium-Tellurium System, ChemInform. 18 (1987) 535–543. https://doi.org/10.1002/chin.198745021.

[70] C.-S. Oh, D.N. Lee, Thermodynamic assessment of the Ga-Te system, Calphad. 16 (1992) 317–330. https://doi.org/10.1016/0364-5916(92)90029-W.

[71] Y. Liu, Z. Dou, M. Enoki, Y. Oyama, H. Ohtani, Calphad Thermodynamic assessment of the Ga–Se–Te system, Calphad. 71 (2020) 102206. https://doi.org/10.1016/j.calphad.2020.102206.

[72] W. Klemm, H.U. v. Vogel, Messungen an Gallium- und Indium-Verbindungen. X. Über die Chalkogenide von Gallium und Indium, Zeitschrift Für Anorg. Und Allg. Chemie. 219 (1934) 45–64. https://doi.org/10.1002/zaac.19342190106.

[73] J.R. DALE, Metallographic Examination of the Phase Diagram of the Gallium-Tellurium System, Nature. 197 (1963) 242–246. https://doi.org/10.1038/197242a0.

[74] F. Alapini, J. Flahaut, M. Guittard, S. Jaulmes, M. Julien-Pouzol, Systeme gallium-tellure, J. Solid State Chem. 28 (1979) 309–319. https://doi.org/10.1016/0022-4596(79)90082-3.

[75] J.G. Antonopoulos, T. Karakostas, G.L. Bleris, N.A. Economou, On the phase diagram of the Ga-Te system in the composition range 55 at % Te, J. Mater. Sci. 16 (1981) 733–738. https://doi.org/10.1007/BF02402790.

[76] H. Tschirner, B. Garlipp, R. Rentzsch, Differential Thermal Analysis of the Binary Systems Gallium-Tellurium and Cobalt-Tellurium, Z. Met. 77 (1986) 811–814. https://scholar.google.com/scholar?cluster=10731010659220450275&hl=en&as_sdt=20

05&sciodt=0,5#.

[77] R. Blachnik, E. Irle, Das System Gallium-Tellur, J. Less Common Met. 113 (1985) L1–L3. https://doi.org/10.1016/0022-5088(85)90158-4.

[78] V.M. Glazov, L.M. Pavlova, Dissociation degree of Ga and In tellurides at melting point use of liquidus curvature data, Izv. Akad. Nauk SSSR, Neorg. Mater. 13 (1977) 217–221. http://inis.iaea.org/Search/search.aspx?orig_q=RN:9391375.

[79] M. Wobst, Verlauf der mischungslücken der binären systeme silber-tellur, indium-tellur, gallium-tellur, thallium-tellur und antimon-selen, Scr. Metall. 5 (1971) 583–585. https://doi.org/10.1016/0036-9748(71)90117-7.

[80] D. Mouani, G. Morgant, B. Legendre, Study of the phase equilibria in the ternary gold gallium tellurium system, J. Alloys Compd. 226 (1995) 222–231. https://doi.org/10.1016/0925-8388(95)01606-6.

[81] C.-H. Su, Partial pressures of Te2 and thermodynamic properties of Ga–Te system, Thermochim. Acta. 390 (2002) 21–29. https://doi.org/10.1016/S0040-6031(02)00061-8.

[82] B. Predel, J. Piehl, M.J. Pool, Thermodynamic investigations on the binary liquid alloys of tellurium with gallium, indium and thallium, Zeitschrift Fuer Met. 66 (1975) 268–274. http://inis.iaea.org/Search/search.aspx?orig_q=RN:7223360.

[83] I. Katayama, J. Nakayama, T. Nakai, Z. Kozuka, Activity Measurements of Liquid Ga–Te and Ga–Sb Alloys by EMF Method with Solid Electrolyte, Trans. Japan Inst. Met. 28 (1987) 129–134. https://doi.org/10.2320/matertrans1960.28.129.

[84] S. Srikanth, K.T. Jacob, Activities in liquid Ga-Te alloys at 1120 K, Thermochim. Acta. 153 (1989) 27–35. https://doi.org/10.1016/0040-6031(89)85419-X.

[85] R. Castanet, C. Bergman, Thermodynamic functions and structure of gallium + tellurium liquid alloys, J. Chem. Thermodyn. 9 (1977) 1127–1132. https://doi.org/10.1016/0021-9614(77)90114-8.

[86] H. Said, R. Castanet, Thermodynamic investigations of liquid and solid Ga-Te alloys, J. Less Common Met. 68 (1979) 213–221. https://doi.org/10.1016/0022-5088(79)90059-6.

[87] S.A. Alfer, L.A. Mechkovski, A.A. Vecher, Determination of the enthalpy of formation of binary and ternary alloys containing a volatile component by a quantitative DTA method, Thermochim. Acta. 88 (1985) 493–496. https://doi.org/10.1016/0040-6031(85)85473-3.

[88] A.S. Abbasov, A. V. Nikol'skaya, Y.I. Gerasimov, V.P. Vasil'ev, The thermodynamic properties of gallium tellurides investigated by the electromotive force method, Dokl. Akad. Nauk SSSR. 156 (1964) 1140–1142. http://mi.mathnet.ru/eng/dan29727.

[89] P.G. Rustamov, N.A. Seidova, M.G. Shakhbazov, GaTe-Bi2Te3 system, Zhurnal Neorg. Khimii. 21 (1976) 860–862. http://inis.iaea.org/Search/search.aspx?orig_q=RN:8329912.

[90] P.G. Rustamov, N.A. Seidova, M.G. Shakhbazov, The Ga-Bi-Te system, Zhurnal Neorg.

Khimii. 21 (1976) 764–768. http://inis.iaea.org/Search/search.aspx?orig_q=RN:8329911.

[91] M.. Shakhbazov, N.A. Seidova, P.G. Rustamov, Isothermal sections at 600, 400 and 200 deg C Ga-Bi-Te system, Zhurnal Neorg. Khimii. 22 (1977) 2543–2548. https://inis.iaea.org/search/searchsinglerecord.aspx?recordsFor=SingleRecord&RN=9388672.

[92] K. Kurosaki, H. Matsumoto, A. Charoenphakdee, S. Yamanaka, M. Ishimaru, Y. Hirotsu, Unexpectedly low thermal conductivity in natural nanostructured bulk Ga2Te3, Appl. Phys. Lett. 93 (2008) 012101. https://doi.org/10.1063/1.2940591.